Tanguy Mertens

A new mapped infinite partition of unity method for convected acoustical radiation in infinite domains.

January 20, 2009

Université Libre de Bruxelles

Remerciements

Si tu donnes un poisson à un homme, il ne mangera qu'un jour. S'il apprend à pêcher, il mangera toute sa vie.

Proverbe de Confucius, repris plus tard par Dominique Pire dans le cadre de l'action Iles de Paix.

Je remercie Philippe Bouillard de m'avoir donné ma canne à pêche et conduit à l'étang. Je remercie Laurent Hazard et Guy Paulus pour tous leurs conseils avisés. Et tous les autres, famille, amis, qui ont gardé confiance en moi et m'ont encouragé à la persévérance.

C'est grâce à vous tous que je peux vous présenter avec fierté mon premier poisson.

Ceci dit, je voudrais remercier de manière plus académique tous les acteurs du projet.

Je remercie Philippe Bouillard qui est à la source du projet et qui a contribué à mon épanouissement scientifique durant cette aventure au sein du service BATir. Je remercie également pour leur encadrement: Guy Warzée pour sa gentillesse et sa patience ainsi que Jean-Louis Migeot pour son soutien industriel et ses remarques pertinentes.

Ce passage au service BATir a été une expérience riche sur le plan scientifique mais aussi humain. Je remercie mes collègues de l'ULB pour les relations que nous avons construites ensemble, pour les activités dans le cadre du travail ou hors des murs de l'université. Je pense évidemment à Laurent Hazard et à Guy Paulus, pour leur amitié mais aussi leur disponibilité et leurs nombreux conseils. Merci aussi à tous les membres du service des milieux continus qui ont ajouté une dimension humaine. La nature des contrats de recherche et d'assistanat est tel qu'ils furent nombreux a être passés par les murs de l'université. Je ne pourrai tous les citer mais je tiens quand même à remercier personellement Katy, Erik, Geneviève, Yannick, Louise, Dominique, Thierry, Sandrine, Bertha, David, Benoît, Peter et Kfir.

S'il est vrai qu'un travail de thèse tend à rendre le chercheur autonome, les collaborations et interactions restent importantes. Je remercie à cet égard toute l'équipe de l'Institute of Sound and Vibration Research de l'université de Southampton. Je remercie Jeremy Astley, chef du service de m'y avoir accueilli pendant un stage de six mois. Je le

remercie aussi pour l'environnement de travail de qualité qu'il m'a offert. Il est évident que la présence de Pablo Gamallo à l'I.S.V.R. a énormément contribué à l'aboutissement de ce travail de recherche. Je le remercie pour tout le temps qu'il m'a consacré, à Southampton et même par la suite lors de contacts e-mail ou lors de rencontres en conférences. Je le remercie pour l'intérêt qu'il porte à la présente étude, pour ses encouragements et pour tous ses enseignements. Mais ce séjour n'a pas été que professionellement enrichissant, je repense à l'accueil qui m'a été réservé ainsi que de nombreux excellents souvenirs qui font de ce séjour une partie inoubliable de ma vie. Je tiens donc à remercier chaleureusement pour leur amitié précieuse Vincent et Theresa, Luigi, Claire, Naoki, Rie, Sue, Lisa, Eugene, Isa, Daniel et Stéphanie, Alessandro et Emmet.

Ces quelques lignes indiquent à quel point les relations humaines ont une influence sur ma vie. Cela ne sera pas une surprise alors si je remercie les personnes pour qui je *travaille dans les avions* ou ceux qui me félicitent de mon travail, *les semaines durant lesquelles, ils n'ont pas trop entendu les avions*. Je pense bien entendu à ma famille, principalement ma maman, pour avoir fait de moi l'homme que je suis aujourd'hui et mes amis, plus particulièrement mes collocataires: Iyad, Mathieu, Quentin, Guerrick, Caroline et Florence. Merci à vous de partager mes valeurs et de colorier mon existence.

Enfin, je terminerai par remercier les deux petits rayons de soleil qui ont ensoleillé la fin de ce long parcours.

List of Symbols

Greek symbols

β : $\sqrt{1 - M_0^2}$
γ : Poisson ratio of specific heat capacities : c_p/c_v
Γ : interface separating the inner and the outer domains
ε : Error
μ : phase function $[m]$
ρ : mass density $[kgm^{-3}]$
ρ_0 : steady mean density $[kgm^{-3}]$
ρ_a : acoustic density $[kgm^{-3}]$
$\boldsymbol{\sigma}$: stress tensor $[Nm^{-2}]$
ϕ : velocity potential $[m^2s^{-1}]$
ϕ_0 : mean velocity potential $[m^2s^{-1}]$
ϕ_a : acoustic velocity potential $[m^2s^{-1}]$
$\tilde{\phi}_a$: amplitude of the harmonic acoustic velocity potential $[m^2s^{-1}]$
$\tilde{\phi}^h$: numerical approximation of $\tilde{\phi}_a$ $[m^2s^{-1}]$
$\tilde{\phi}_h^I$: numerical approximation in the outer region Ω_o $[m^2s^{-1}]$
Φ_α : shape function for the α^{th} degree of freedom
Φ_α^I : infinite shape function for the α^{th} degree of freedom
ω : angular frequency $[s^{-1}]$
Ω : domain
Ω_i : inner region
Ω_o : outer region

Arabic symbols

$\tilde{a}_n$	: normal acceleration of a vibrating wall	$[ms^{-2}]$
A_n	: normal acoustic admittance	$[m^2skg^{-1}]$
$A_{mn}^{\pm}$	: incident and reflected modal amplitude	$[m^2s^{-1}]$
c	: speed of sound	$[ms^{-1}]$
c_0	: steady mean part of the speed of sound	$[ms^{-1}]$
c_∞	: speed of sound at large distance from the source	$[ms^{-1}]$
c_p	: specific heat capacity at constant pressure	$[JK^{-1}]$
c_v	: specific heat capacity at constant volume	$[JK^{-1}]$
$dofs$	: number of unknowns of the approximation	
E	: energy flow out of a surface	$[J]$
$E_{mn}^{\pm}$	: incident and reflected modal patern	
f	: excitation frequency	$[s^{-1}]$
G	: geometric factor	
h	: mesh size	$[m]$
H	: Hilbert space	
i	: imaginary unit $= \sqrt{-1}$	
$\mathbf{I}$	: Sound intensity	$[Wm^{-2}]$
J'	: stagnation entropy	$[Jkg^{-1}]$
k	: wavenumber	$[m^{-1}]$
$k_{r,mn}^{\pm}$	: incident and reflected radial wavenumber	$[m^{-1}]$
k_B	: Boltzmann constant	$[JK^{-1}]$
$K_{z,mn}^{\pm}$	: incident and reflected axial wavenumber	$[m^{-1}]$
L_j^d	: Legendre polynomial of order d for node j	
L_s	: curve enclosing the boundary S_s	
L_v	: curve enclosing the boundary S_v	
m	: angular mode number	
$\mathbf{m}'$	: mass flux	$[kgm^-2s^{-1}]$
m_0	: radial order of the infinite element	
m_w	: mass of a molecule	$[kg]$
M_0	: mach number	
M_i	: Mapping function for node/point i	
$\mathbf{n}$	: outer normal to the domain	
n	: radial mode number	
n_d^I	: number of infinite degree of freedom	
$n\,(j)$	: size of the local approximation space at node j	
nni	: number of infinite nodes	
$nodes$	: number of nodes	
N_i	: Partition of Unity function of node i	
N_m	: number of angular modes	
N_n	: number of radial modes	
N_M	: number of reflected modes (unknown)	

p	: fluid pressure	$[Pa]$
p_0	: steady mean fluid pressure	$[Pa]$
p_a	: acoustic pressure	$[Pa]$
$\tilde{p}_a$	: amplitude of the harmonic acoustic pressure	$[Pa]$
$\tilde{p}_{an}$	: analytic amplitude of the harmonic acoustic pressure	$[Pa]$
$\mathbf{q}$	: heat flux	$[Wm^{-2}]$
Q_w	: heat production	$[J]$
r_o	: distance to the source point	$[m]$
R	: specific gas constant	$[JK^{-1}mol^{-1}]$
R_j	: radial function for infinite node j	
R_j^d	: radial function of order d for node j	
s	: entropy	$[Jkg^{-1}K^{-1}]$
S	: boundary	
S_i	: mapping functions for the interface Γ	
S_M	: Modal boundary	
S_s	: soft wall	
S_v	: vibrating wall	
t	: time	$[s]$
T	: Temperature	$[K]$
T_j	: circumferential function for infinite node j	
$\tilde{u}_n$	: normal displacement of a vibrating wall	$[m]$
$\mathbf{v}$	: fluid velocity	$[ms^{-1}]$
$\mathbf{v}_0$	: steady mean fluid velocity	$[ms^{-1}]$
$\mathbf{v}_\infty$	: fluid velocity at large distance from the source	$[ms^{-1}]$
$\mathbf{v}_a$	: acoustic velocity	$[ms^{-1}]$
$\tilde{\mathbf{v}}_a$	: amplitude of the harmonic acoustic velocity	$[ms^{-1}]$
$\mathscr{V}$	: the Sobolev space $W^{1,2} = H^1 = \{f : f, \nabla f \in L^2\}$	
V_{jl}	: l^{th} local approximation function of node j	
$\tilde{w}_n$	: normal velocity of a vibrating wall	$[ms^{-1}]$
W_j	: weight function of node j	
W_j^I	: infinite weight function of the infinite node j	
$W_{M,nm}$	: modal weight function of the angular and radial mode (m, n)	

Operators

∇	: gradient operator
$\nabla\cdot$	: divergence operator
$\nabla\times$	: curl operator
Δ	: Laplacian operator
$\frac{D}{Dt}$	: Total time derivative
:	: the double dot product of two tensors
$\langle\ \rangle$	: time average
$\Re$	: Real part

Contents

10

Appendices

10.1 Mapping functions

10.1.1 Three-dimensional mapping

Finite elements

Mapping functions for the vertices ($\xi_0 = \xi\xi_i$ and ξ_i is the local coordinates of the node i.):

$$M_i(\xi,\eta,\zeta) = \frac{1}{8}(1+\xi_0)(1+\eta_0)(1+\zeta_0)(\xi_0+\eta_0+\zeta_0-2) \tag{10.1}$$

The mapping functions for the mid-side points (mapping points):

$$\begin{aligned} M_i(\xi,\eta,\zeta) &= \frac{1}{4}\left(1-\xi^2\right)(1+\eta_0)(1+\zeta_0) \;\; for\, \xi_i = 0 \\ M_i(\xi,\eta,\zeta) &= \frac{1}{4}(1+\xi_0)\left(1-\eta^2\right)(1+\zeta_0) \;\; for\, \eta_i = 0 \\ M_i(\xi,\eta,\zeta) &= \frac{1}{4}(1+\xi_0)(1+\eta_0)\left(1-\zeta^2\right) \;\; for\, \zeta_i = 0 \end{aligned} \tag{10.2}$$

Infinite elements

The infinite mapping is based on 16 mapping functions, corresponding to the location of 16 mapping points : the 4 base nodes and the four base mapping points (where 'base' means lying on the interface Γ) and their mapping points located at twice the distance from the source points (which corresponds to the ordinate $\zeta_i = 0$).

The mapping functions for the points on the corners of the infinite element lying on the interface Γ : ($\zeta_i = -1$) and $(\xi_i, \eta_i) = (\pm 1, \pm 1)$:

$$M_i(\xi,\eta,\zeta) = \frac{1}{4}(1+\xi_0)(1+\eta_0)(\xi_0+\eta_0-1)\left(\frac{-2\zeta}{1-\zeta}\right) \;\; with\; i = 1:4 \tag{10.3}$$

The mapping functions for the points on the mid-side of the base of the infinite element: $(\zeta_i = -1)$ and $(\xi_i, \eta_i) = (0, \pm 1)$ given at equation 10.4 or $(\xi_i, \eta_i) = (\pm 1, 0)$ given at equation 10.5:

$$M_i(\xi, \eta, \zeta) = \frac{1}{2}\left(1 - \xi^2\right)(1 + \eta_0)\left(\frac{-2\zeta}{1 - \zeta}\right) \quad with\ i = 5, 7 \tag{10.4}$$

$$M_i(\xi, \eta, \zeta) = \frac{1}{2}\left(1 - \eta^2\right)(1 + \xi_0)\left(\frac{-2\zeta}{1 - \zeta}\right) \quad with\ i = 6, 8 \tag{10.5}$$

The mapping functions for the points of the infinite element for which $(\zeta_i = 0)$ and $(\xi_i, \eta_i) = (\pm 1, \pm 1)$:

$$M_i(\xi, \eta, \zeta) = \frac{1}{4}(1 + \xi_0)(1 + \eta_0)(\xi_0 + \eta_0 - 1)\left(\frac{1 + \zeta}{1 - \zeta}\right) \quad with\ i = 9 : 12 \tag{10.6}$$

The mapping functions for the points on the mid-side at $(\zeta_i = 0)$ and $(\xi_i, \eta_i) = (0, \pm 1)$ given at equation 10.7 or $(\xi_i, \eta_i) = (\pm 1, 0)$ given at equation 10.8:

$$M_i(\xi, \eta, \zeta) = \frac{1}{2}\left(1 - \xi^2\right)(1 + \eta_0)\left(\frac{1 + \zeta}{1 - \zeta}\right) \quad with\ i = 13, 15 \tag{10.7}$$

$$M_i(\xi, \eta, \zeta) = \frac{1}{2}\left(1 - \eta^2\right)(1 + \xi_0)\left(\frac{1 + \zeta}{1 - \zeta}\right) \quad with\ i = 14, 16 \tag{10.8}$$

10.1.2 Two-dimensional mapping

Finite elements

Mapping functions for the 4 vertices:

$$M_i(\xi, \eta) = \frac{1}{4}(1 + \xi_0)(1 + \eta_0)(\xi_0 + \eta_0 - 1) \tag{10.9}$$

where $\xi_0 = \xi\xi_i$ and ξ_i is the local coordinates of the node i.

The mapping functions for 4 the mid-side points (mapping points)

$$\begin{aligned} M_i(\xi, \eta) &= \frac{1}{2}\left(1 - \xi^2\right)(1 + \eta_0) \ \ for\ \xi_i = 0 \\ M_i(\xi, \eta) &= \frac{1}{2}(1 + \xi_0)\left(1 - \eta^2\right) \ \ for\ \eta_i = 0 \end{aligned} \tag{10.10}$$

Infinite elements

The infinite mapping is based on 6 mapping functions, corresponding to the location of 6 mapping points : the 2 base nodes and the base mapping point (where 'base' means

lying on the interface Γ) and their mapping points located at twice the distance from the source points (which corresponds to the ordinate $\zeta_i = 0$).

The mapping functions for the nodes of the infinite element lying on the interface Γ: $(\xi_i, \eta_i) = (\pm 1, -1)$:

$$M_i(\xi, \eta) = \left(\xi^2 + \xi_0\right)\left(\frac{-\eta}{1-\eta}\right) \; with\; i = 1:2 \tag{10.11}$$

The mapping functions for the point on the mid-side of the base of the infinite element: $(\xi_i, \eta_i) = (0, -1)$ given at equation 10.12:

$$M_i(\xi, \eta) = \left(1 - \xi^2\right)\left(\frac{-\eta}{1-\eta}\right) \; with\; i = 3 \tag{10.12}$$

The mapping functions for the points of the infinite element for which $(\xi_i, \eta_i) = (\pm 1, 0)$:

$$M_i(\xi, \eta) = \frac{1}{2}\left(\xi^2 + \xi_0\right)\left(\frac{1+\eta}{1-\eta}\right) \; with\; i = 4:5 \tag{10.13}$$

The mapping functions for the points on the mid-side at $(\zeta_i = 0)$ and $(\xi_i, \eta_i) = (0, 0)$ given at equation 10.14:

$$M_i(\xi, \eta) = \left(1 - \xi^2\right)\left(\frac{1+\eta}{1-\eta}\right) \; with\; i = 6 \tag{10.14}$$

10.2 Modes in a two-dimensional lined duct with uniform mean flow along the duct axis

We consider a two-dimensional infinite duct composed of a hard wall at the lower wall of the duct ($y = 0$) and of a liner for the upper part ($y = h$). In this special case, the convected wave equation becomes after the decomposition of variables $\tilde{\phi}_a = \phi_x \phi_y$, where x is the axial direction:

$$\begin{cases} \beta^2 \frac{\partial^2 \phi_x}{\partial x^2} - 2ikM \frac{\partial \phi_x}{\partial x} + k_x^2 \phi_x = 0 \\ \frac{\partial^2 \phi_y}{\partial y^2} + k_y^2 \phi_y = 0 \\ k^2 = k_x^2 + k_y^2 \end{cases} \tag{10.15}$$

The solution in the x axis can be compared to equation 2.71 as they are solutions of the same equation:

$$\begin{cases} \phi_x = A^+ e^{-iK_x^+ x} + A^- e^{-iK_x^- x} \\ K_x^\pm = \frac{-kM_0 \mp \sqrt{k^2 - \beta^2 k_y^{\pm 2}}}{\beta^2} \end{cases} \tag{10.16}$$

The acoustic modes propagating in the duct are obtained by solving equation 10.15 in the y direction and taking into account the effect of the soft wall 2.38. This leads to:

$$\begin{cases} \phi_y = Ae^{-ik_y^+ y} + Be^{-ik_y^- y} \\ k_y^\pm \tan\left(k_y^\pm h\right) = iA_n\rho_0 c_0 k - 2iA_n\rho_0 c_0 M_0 \left(1 - \frac{M_0}{2k} K_x^\pm\right) K_x^\pm \end{cases} \tag{10.17}$$

The value of the wavenumbers is obtained by solving equations 10.16 and 10.17. This can be done iteratively.

In the case of lined wall and non-zero mean flow, the wavenumbers of the right traveling waves $\left(k_y^+, K_x^+\right)$ are different from those of the left ones $\left(k_y^-, K_x^-\right)$, while in other cases (hard-wall + flow, hard-wall + no-flow or soft-wall + no-flow) the 'radial' wavenumbers $k_y^\pm$ are the same for the left and right traveling modes.

10.3 Outwardly propagating wavelike factor

The convected wave equation can be re-written for the case of a uniform one-dimensional flow oriented along the x axis ($\mathbf{v}_0 = v_0\mathbf{1}_x$ and $M_0 = v_0/c_0$):

$$\left(\frac{1}{c_0}\frac{\partial}{\partial t} + M_0\frac{\partial}{\partial x}\right)^2 \phi_a - \nabla^2\phi_a = 0 \tag{10.18}$$

where $\beta^2 = 1 - M_0^2$ and ϕ_a the instantaneous acoustic pressure.

The following transformation [35] allow to re-write the convected wave equation to a simpler form 10.19.

$$\begin{cases} x' = \frac{x}{\beta} \\ y' = y \\ z' = z \\ t' = \beta t + \frac{M_0 x}{\beta^2 c_0} \end{cases}$$

$$\left(\frac{1}{c_0^2}\frac{\partial'^2}{\partial t'^2} + \nabla'^2\right)\phi_a = 0 \tag{10.19}$$

Expression 10.20 is solution of the modified convected wave equation.

$$\phi_a\left(\mathbf{x}', t'\right) = e^{\frac{i\omega t'}{\beta}} \frac{e^{\frac{-ik}{\beta}\sqrt{x'^2+y'^2+z'^2}}}{\sqrt{x'^2+y'^2+z'^2}} \tag{10.20}$$

This corresponds to:

$$\phi_a(\mathbf{x},t) = e^{i\omega t} e^{\frac{ikM_0x}{\beta^2}} \frac{e^{\frac{-ik}{\beta}\sqrt{\frac{x^2}{\beta^2}+y^2+z^2}}}{\sqrt{\frac{x^2}{\beta^2}+y^2+z^2}} \tag{10.21}$$

Then we regroup spacial $\mathbf{x}$ terms in the wavelike factor μ:

$$e^{-ik\mu(\mathbf{x},\mathbf{M_0})} = e^{-ik\left(-\frac{M_0x}{\beta^2}+\frac{1}{\beta^2}\sqrt{x^2+\beta^2(y^2+z^2)}\right)} \tag{10.22}$$

To ensure continuity of the potential across the interface Γ, the wavelike factor $\mu(\mathbf{x}, M_0)$ is taken equal to 0 for $\zeta = -1$. The wavelike factor is then expressed in parent coordinates:

$$\begin{aligned}\mu\ (\mathbf{x}, M_0) = &\sum_{i=1}^{8} \frac{S_i(\xi,\eta)}{\beta^2}\left(\frac{1+\zeta}{1-\zeta}\right) \\ &\left(-M_0(x_i - x_i') + \sqrt{(x_i-x_i')^2 + \beta^2\left((y_i-y_i')^2 + (z_i-z_i')^2\right)}\right)\end{aligned} \tag{10.23}$$

with x_i, y_i, z_i and x_i', y_i', z_i' being respectively the coordinates of the nodes and mapping points (lying on the interface Γ) and the source points.

10.4 Effect of uniform mean flow on plane wave propagation

Considering the general case of a plane wave propagating in a free domain:

$$\tilde{\phi}_a = Ae^{ik_xx}e^{ik_yy} \tag{10.24}$$

We consider an infinite plane without any object which could modify the propagation. The flow is assumed to be uniform. The direction of the constant mean flow velocity of amplitude v_0 is given by angle β such that:

$$\begin{aligned} v_x &= v_0 cos(\beta) \\ v_y &= v_0 sin(\beta) \end{aligned} \tag{10.25}$$

Using these assumptions in the two-dimensional convected wave equation for a wave propagating with a wavenumber $k = \sqrt{k_x^2 + k_y^2}$ leads to:

$$\begin{aligned} &-k_x^2 - k_y^2 + M^2 cos^2(\beta) k_x^2 + M^2 sin^2(\beta) k_y^2 - \\ &2kM cos(\beta) k_x - 2kM sin(\beta) k_y \\ &2M^2 cos(\beta) sin(\beta) k_x k_y + k^2 = 0 \end{aligned} \tag{10.26}$$

If, for instance, the uniform mean flow is along x ($\beta = 0$), this equation is simplified:

$$k^2 = k_y^2 + \left(1 - M^2\right) k_x^2 + 2kMk_x \tag{10.27}$$

The above equation defines an ellipse (figure 10.1) aligned with the flow direction in the (k_x, k_y) plane. The parametric equation is given by:

$$\frac{k_x}{k} = \frac{cos\,(\theta)}{1 + Mcos\,(\theta)} \tag{10.28}$$

$$\frac{k_y}{k} = \frac{sin\,(\theta)}{1 + Mcos\,(\theta)} \tag{10.29}$$

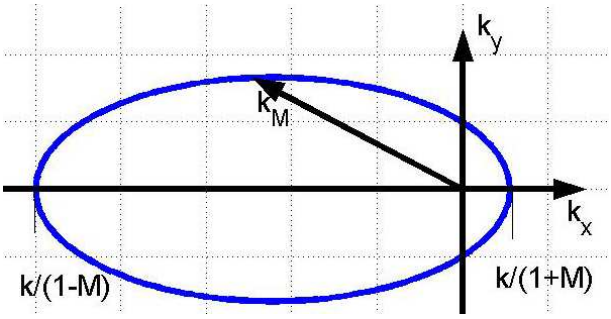

Fig. 10.1. Influence of a flow along x on the physical wavenumber

If θ and β vary, the general wave number is given by:

$$k_M = k\frac{1}{1 + Mcos\,(\theta - \beta)} \tag{10.30}$$

where k_M is the effective wavenumber by taking into account the mean flow.

The equation (10.30) means that the mean flow velocity and the orientation between the wave and the flow has an effect on wave propagation. As a consequence, a wave propagating in a convected medium does not exhibit a wavenumber corresponding to the excitation frequency. This remark has to be taken into account to determine the size of the elements. In convected wave propagation, the rule of the thumb is still a reference. However, the wavelength which has to be used in the rule must be the smallest wavelength. The mesh has to represent the propagation of the physical wave. The physical wavenumber can vary a lot from the one related to the excitation frequency, especially for high mach numbers. For example, if $M = 0.8$, there is a factor 10 between the upstream and the downstream wavenumbers.

10.5 Local enrichment: Application to the multipole

The aim of locally enriched nodes is to improve the approximation without generating a new mesh. This section illustrates local enrichment for the radiation of a multipole (N=7) at 700Hz. For this application, there is no particular regions to enrich (no flow, no edges). The radiation is quite the same in the whole domain. We decided to analyse a uniform pressure distribution problem. We selected two ways of enriching the nodes. The first one selects the nodes whose distance to the origin is lower than r_1 (scheme1: figure 10.2(a)). The other selects nodes at a larger distance than r_2 (scheme2: figure 10.2(b)). At the origin, enrichment functions are of order p=0. Selected nodes will be enriched with non complete polynomial functions $p = 2-\{zr\}$[1]. Figure 10.3 illustrates the evolution of the L_2 norm with respect to the number of degrees of freedom. This figure shows classic convergence curves: uniform enrichment ($p = 0$ and $p = 2 - \{zr\}$) over the domain, each point correspond to a given mesh. The other curves correspond to a given mesh with varying the enrichment following scheme1 or scheme2. Both meshes considered for this application corresponds to n elements in the radial direction and n elements in the circumferential one with $n = 20$ and 40.

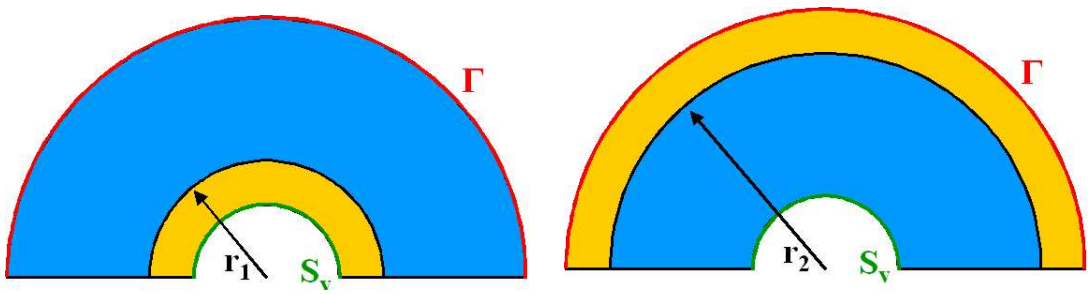

(a) (a)

Fig. 10.2. Illustration of the selection of the nodes to enrich: (a) scheme1 - (b) scheme2 . The region with $p = 0$ is in blue, the one with $p = 2 - \{zr\}$ in orange.

Figure 10.3 shows that locally enriched nodes significantly improve the accuracy of the solution. Even if there is no particular reason to enrich one region compared to another regarding the uniform pressure distribution, it can be observed in figure 10.3 that it is slightly better to enrich nodes close to the source. In this case the best improvement in accuracy is obtained for high number of nodes enriched with $p = 2 - \{zr\}$.

[1] We also made simulations with complete polynomials of order 2. We noticed that, on a same mesh, the accuracy was the same with the complete and the non complete sets. We then decided to continue with the non complete enrichment as for the same mesh, it leads to lower degrees of freedom than the complete one.

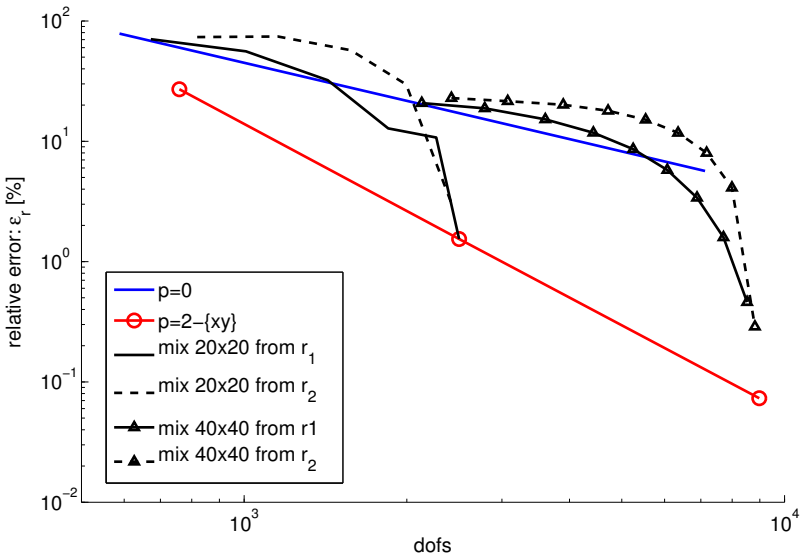

Fig. 10.3. Multipole (m=0,n=7) radiation at 700 Hz : evolution of the L_2 norm with respect to the number of degrees of freedom.

References

1. Ph. Bouillard, F. Ihlenburg, Error estimation and adaptivity for the finite element solution in acoustics: 2D and 3D applications, Comput. Methods Appl. Mech. Engrg. 176 (1999) 147-163.
2. F. Ihlenburg, I. Babuška, Dispersion analysis and error estimation of Galerkin finite element methods for the Helmholtz equation, Int. J. Numer. Methods Eng. 38 (1995) 3745-3774.
3. J.T. Oden, S. Prudhomme, L. Demkowicz, A posteriori error estimation for acoustic wave propagation problems, Arch. Comput. Meth. Engng. 12 (2005) 343-389.
4. F. Ihlenburg, I. Babuška, Finite element solution of the Helmholtz equation with high wave number part II : the h-p version of the FEM, SIAM J. Numer. Anal. 34 (1997) 315-358.
5. O.C. Zienkiewicz, Achievements and some unsolved problems of the finite element method, Int. J. Numer. Methods Eng. 47 (2000) 9-28.
6. L.L. Thompson, A review of finite element methods for time-harmonic acoustics, J. Acoust. Soc. Am. 119 (2006) 1315-1330.
7. J.M. Melenk, I. Babuška, The partition of unity finite element method: basic theory and applications, Comput. Methods Appl. Mech. Engrg. 139 (1996) 289-314.
8. I. Babuška, J.M. Melenk, The Partition of Unity Method, Int. J. Numer. Methods Eng. 40 (1997) 727-758.
9. O. Laghrouche, P. Bettess, R. J. Astley, Modeling of short wave diffraction problems using approximating systems of plane waves, Int. J. Numer. Methods Eng. 54 (2002) 1501-1533.
10. Th. Strouboulis, I. Babuška, R. Hidajat, The generalized finite element method for Helmholtz equation: Theory, computation, and open problems, Comput. Methods Appl. Mech. Engrg. 195 (2006) 4711-4731.
11. Th. Strouboulis, R. Hidajat, I. Babuška, The generalized finite element method for Helmholtz equation Part II: Effect of choice of handbook functions, error due to absorbing boundary conditions and its assessment, Comput. Methods Appl. Mech. Engrg. 197 (2008) 364-380.
12. Th. Strouboulis, K. Copps, I. Babuška, The generalized finite element method, Comput. Methods Appl. Mech. Engrg. 190 (2001) 4081-4193.
13. Th. Strouboulis, I. Babuška, K. Copps, The design and analysis of the generalized finite element method, Comput. Methods Appl. Mech. Engrg. 181 (2000) 43-69.
14. C. Farhat, I. Harari, L.P. Franca, The discontinuous enrichment method, Comput. Methods Appl. Mech. Engrg. 190 (2001) 6455-6479.
15. B. Pluymers, W. Desmet, D. Vandepitte, P. Sas, Application of an efficient wave-based prediction technique for the analysis of vibro-acoustic radiation problems, J. Comput. Appl. Math. 168 (2004) 353-364.
16. P. Gamallo, R.J. Astley, A comparison of two Trefftz-type methods: The ultraweak variational formulation and the least-squares method, for solving shortwave 2-D Helmholtz problems, Int. J. Numer. Methods Eng. 71 (2007) 406-432.
17. P. Gamallo, R.J. Astley, The partition of unity finite element method for short wave acoustic propagation on non-uniform potential flows, Int. J. Numer. Methods Eng. 65 (2006) 425-444.
18. T. Huttunen, P. Gamallo, R.J. Astley, Comparison of two wave element methods for the Helmholtz problem, Commun. Numer. Meth. Engng. Article in Press (2008) doi:10.1002/cnm1102.
19. T. Huttunen, P. Monk, J.P. Kaipio, Computational aspects of the ultra weak variational formulation, J. Comput. Phys. 182 (2002) 27-46.
20. T. Huttunen, J.P. Kaipio, P. Monk, An ultra weak method for acoustic fluid-solid interaction, J. Comput. Appl Math. 213 (2008) 166-185.

21. P. Monk, D.-Q. Wang, A least squares method for the Helmholtz equation, Comput. Methods Appl. Mech. Engrg. 175 (1999) 121-136.
22. R. Sevilla, S. Fernández-Méndez, A. Huerta, NURBS-enhanced finite element method (NEFEM), Int. J. Numer. Methods Eng. Early ViewW (2008) doi: 10.1002/nme.2311
23. E. Chadwick, P. Bettess, O. Laghrouche, Diffraction of short waves modeled using new mapped wave envelope finite and infinite elements, Int. J. Numer. Methods Eng. 45 (1999) 335-354.
24. E. De Bel, P. Villon, Ph. Bouillard, Forced vibrations in the medium frequency range solved by a partition of unity method with local information, Int. J. Numer. Methods Eng. 162 (2004) 1105-1126.
25. L. Hazard, Ph. Bouillard, Structural dynamics of viscoelastic sandwich plates by the partition of unity finite element method, Comput. Methods Appl. Mech. Engrg. 196 (2007) 4101-4116.
26. T.J.R. Hughes, J.A. Cotrell, Y. Bazilevs, Isogeometric analysis: CAD, finite elements, NURBS, exact geometry and mesh refinement, Comput. Methods Appl. Mech. Engrg. 194 (2005) 4135-4195.
27. B. Szabó, A. Düster, E. Rank, The p-version of the finite element method, in: E. Stein, R. de Borst, T.J.R. Hughes (Eds.), Fundamentals, Encyclopedia of Computational Mechanics, vol. 1, Wiley, New York, 2004 (Chapter 5).
28. R.J. Astley, P. Gamallo, Special short wave elements for flow acoustics, Comput. Methods Appl. Mech. Engrg. 194 (2005) 341-353.
29. R.J. Astley, P. Gamallo, The Partition of Unity Finite Element Method for Short Wave Acoustic Propagation on Non-uniform Potential Flows, Int. J. Numer. Methods Eng. 65 (2006) 425-444.
30. R.J. Astley, G.J. Macaulay, J.-P. Coyette, L. Cremers, Three-dimensional wave-envelope elements of variable order for acoustic radiation and scattering. Part I. Formulation in the frequency domain, J. Acoust. Soc. Am. 103 (1998) 49-63.
31. R.J. Astley, J.-P. Coyette, Conditioning of infinite element schemes for wave problems, Commun. Numer. Meth. Engng. 17 (2001) 31-41.
32. D. Dreyer, O. von Estorff, Improved conditioning of infinite elements for exterior acoustics, Int. J. Numer. Methods Eng. 58 (2003) 933-953.
33. J.J. Shirron, I. Babuška, A comparison of approximate boundary conditions and infinite element methods for exterior Helmholtz problems, Comput. Methods Appl. Mech. Engrg. 164 (1998) 121-139
34. D. Dreyer, Efficient infinite elements for exterior acoustics, PhD thesis, Shaker Verlag, Aachen, 2004.
35. W. Eversman, Mapped infinite wave envelope elements for acoustic radiation in a uniformly moving medium, J. Sound Vib. 224 (1999) 665-687.
36. S.J. Rienstra, W. Eversman, A numerical comparison between the multiple-scales and finite-element solution for sound propagation in lined flow ducts, J. Fluid Mech. 437 (2001) 367-384.
37. S.J. Rienstra, Sound transmission in slowly varying circular and annular lined ducts with flow, J. Fluid Mech. 380 (1999) 279-296.
38. S.J. Rienstra, The Webster equation revisited, 8th AIAA/CEAS Aeroacoustic conference (2002) AIAA 2002-2520.
39. M.K. Myers, On the acoustic boundary condition in the presence of flow, J. Sound Vib. 71 (1980) 429-434.
40. T. Mertens, Meshless modeling of acoustic radiation in infinite domains, Travail de spécialisation, Université Libre de Bruxelles (U.L.B.), 2005.
41. W. Eversman, The boundary condition at an impedance wall in a non-uniform duct with potential mean flow, J. Sound Vib. 246 (2001) 63-69.
42. B. Regan, J. Eaton, Modeling the influence of acoustic liner non-uniformities on duct modes, J. Sound Vib. 219 (1999) 859-879.
43. H.-S. Oh, J.G. Kim, W.-T. Hong, The Piecewise Polynomial Partition of Unity Functions for the Generalized Finite Element Methods, Comput. Methods Appl. Mech. Engrg. Accepted manuscript (2008), doi: 10.1016/j.cma.2008.02.035.
44. Free Field Technologies, Actran user's manual, http://fft.be.
45. University of Florida, Department of Computer and Information Science and Engineering, http://www.cise.ufl.edu/research/sparse/umfpack/
46. T.A. Davis, A column pre-ordering strategy for the unsymmetric-pattern multifrontal method, ACM Transactions on Mathematical Software 30 (2004) 165-195.
47. T.A. Davis, Algorithm 832: UMFPACK, an unsymmetric-pattern multifrontal method, ACM Transactions on Mathematical Software 30 (2004) 196-199.
48. T.A. Davis and I.S. Duff, A combined unifrontal/multifrontal method for unsymmetric sparse matrices, ACM Transactions on Mathematical Software 25 (1999) 1-19.

49. T.A. Davis and I.S. Duff, An unsymmetric-pattern multifrontal method for sparse LU factorization, SIAM Journal on Matrix Analysis and Applications 18 (1997) 140-158.
50. A. Hirschberg, S.W. Rienstra, An introduction to aeroacoustics, Eindhoven University of Technology (2004).
51. G. Warzée, Mécanique des solides et des fluides, Université Libre de Bruxelles (2005).
52. M.J. Crocker, Handbook of acoustics, Wiley-Interscience, New York (1998).
53. R. Sugimoto, P. Bettess, J. Trevelyan, A numerical integration scheme for special quadrilateral finite elements for the helmholtz equation, Commun. Numer. Meth. Engng. 19 (2003) 233-245.
54. G. Gabard, R.J. Astley, A computational mode-matching approach for sound propagation in three-dimensional ducts with flow, J. Sound Vib. Article in Press (2008) doi:10.1016/j.jsv.2008.02.015.
55. C. Farhat, I. Harari, U. Hetmaniuk, A discontinuous Galerkin method with Lagrange multipliers for the solution of Helmholtz problems in the mid-frequency regime, Comput. Methods Appl. Mech. Engrg. 192 (2003) 1389-1419.
56. C.L. Morfey, Acoustic energy in non-uniform flows, J. Sound Vib. 14 (1971) 159-170.
57. F. Magoules, I. Harari (editors), Special issue on Absorbing Boundary Conditions, Comput. Methods Appl. Mech. Engrg. 195 (2006) 3354-3902.
58. M. Fischer, U. Gauger, L. Gaul, A multipole Galerkin boundary element method for acoustics, Engineering Analysis with Boundary Elements 28 (2004) 155-162.
59. J.-P. Bérenger, Three-dimensional Perfectly Matched Layer for the absorption of electromagnetic waves, J. Comput. Phys. 127 (1996) 363-379.
60. C. Michler, L. Demkowicz, J. Kurtz, D. Pardo, Improving the performance of Perfectly Matched Layers by means of hp-adaptivity, Numerical Methods for Partial Differential Equations 23 (2007) 832-858.
61. A. Bayliss, E. Turkel, Radiation boundary conditions for wave-like equations, Comm. Pure Appl. Math. 33 (1980) 707-725.
62. B. Engquist, A. Majda, Radiation boundary conditions for acoustic and elastic wave calculations, Comm. Pure Appl. Math. 32 (1979) 313-357.
63. K. Feng, Finite element method and natural boundary reduction, Proceedings of the International Congress of Mathematicians, Warsaw (1983) 1439-1453.
64. D. Givoli, B. Neta, High-order non-reflecting boundary scheme for time-dependent waves, J. Comput. Phys. 186 (2003) 24-46.
65. T. Hagstrom, A. Mar-Or, D. Givoli, High-order local absorbing conditions for the wave equation: Extensions and improvements, J. Comput. Phys. 227 (2008) 3322-3357.
66. T. Hagstrom, T. Warburton, A new auxiliary variable formulation of high-order local radiation boundary conditions: corner compatibility conditions and extensions to first order systems, Wave Motion 39 (2004) 327-338.
67. A. Hirschberg, S.W. Rienstra, An introduction to aeroacoustics, Eindhoven university of technology (2004).
68. V. Lacroix, Ph. Bouillard, P. Villon, An iterative defect-correction type meshless method for acoustics, Int. J. Numer. Meth. Engng 57 (2003) 2131-2146.
69. T. Mertens, P. Gamallo, R. J. Astley, Ph. Bouillard, A mapped finite and infinite partition of unity method for convected acoustic radiation in axisymmetric domains, Comput. Methods Appl. Mech. Engrg. 197 (2008) 4273-4283.
70. G. Gabard, Discontinuous Galerkin methods with plane waves for time harmonic problems, J. Comput. Phys. 225 (2007) 1961-1984.
71. L. Hazard, Design of viscoelastic damping for vibration and noise control: modeling, experiments and optimisation, PhD thesis, Univesité Libre de Bruxelles (2007).
72. G. Gabard, R.J. Astley, M. Ben Tahar, Stability and accuracy of finite element methods for flow acoustics. I: general theory and application to one-dimensional propagation, Int. J. Numer. Meth. Eng. 63, (2005) 947-973.
73. G. Gabard, R.J. Astley, M. Ben Tahar, Stability and accuracy of finite element methods for flow acoustics. II: Two-dimensional effects, Int. J. Numer. Meth. Eng. 63 (2005) 974-987.
74. A. Goldstein, Steady state unfocused circular aperture beam patterns in non attenuating and attenuating fluids, J. Acoust. Soc. Am. 115 (2004) 99-110.
75. T. Douglas Mast, F. Yu, Simplified expansions for radiation from baffled circular piston, J. Acoust. Soc. Am. 118 (2005) 3457-3464.
76. T. Hasegawa, N. Inoue, K Matsuzawa, A new rigorous expansion for the velocity potential of a circular piston source, J. Acoust. Soc. Am. 74 (1983) 1044-1047.
77. R.J. Astley, A finite element, wave envelope formulation for acoustical radiation in moving flows, J. Sound Vib. 103 (1985) 471-485.
78. J.M. Tyler, T.G. Sofrin, Axial flow compressor noise studies, SAE Transactions 70 (1962) 309-332.

79. M.C. Duta, M.B. Giles, A three-dimensional hybrid finite element/spectral analysis of noise radiation from turbofan inlets, J. Sound Vib. 296 (2006) 623-642.
80. H.H. Brouwer, S.W. Rienstra, Aeroacoustics research in Europe: The CEAS-ASC report on 2007 highlights, J. Sound Vib. Article in Press (2008) doi:10.1016/j.jsv.2008.07.020.
81. http://en.wikipedia.org/wiki/Aircraft_noise, 4th September 2008.
82. Y. Park, S. Kim, S. Lee, C. Cheong, Numerical investigation on radiation characteristics of discrete-frequency noise from scarf and scoop aero-intakes, Appl. Acoust. Article in press (2008) doi:10.1016/j.apacoust.2007.09.005.
83. General Electric Company, http://www.ge.com, http://www.turbokart.com/about_ge90.htm, 4th September 2008.
84. R.J. Astley, J.A. Hamilton, Modeling tone propagation from turbofan inlets - The effect of extended lip liner, AIAA paper 2002-2449 (2002).
85. V. Decouvreur, Updating acoustic models: a constitutive relation error approach, PhD thesis, Université Libre de Bruxelles (2008).
86. P.A. Nelson, O. Kirkeby, T. Takeuchi, and H. Hamada, Sound fields for the production of virtual acoustic images, Letters to the editor, J. Sound Vib. 204 (1999) 386-396.
87. Y. Reymen, W. De Roeck , G. Rubio, M. Bealmans, W. Desmet, A 3D Discontinuous Galerkin Method for aeroacoustic propagation, Proceedings of the 12th International Congress on Sound and Vibration 2005.
88. G. Gabard, Exact integration of polynomial-exponential products with an application to wave based numerical methods, Commun. Numer. Meth. Engng (2008) doi: 10.1002/cnm.1123.
89. New York University, http://math.nyu.edu/faculty/greengar/shortcourse_fmm.pdf, 1st december 2008.